Reduction of Substituted Benzenediazonium Salts by Hydrogen Atoms in Aqueous Acidic Solution Studied by Pulse Radiolysis

Kim Daasbjerg*,† and Knud Sehested‡,§

Department of Chemistry, University of Aarhus, Langelandsgade 140, DK-8000 Aarhus C, Denmark, and Risø National Laboratory, Roskilde, Denmark

Received: November 1, 2002; In Final Form: February 21, 2003

A pulse radiolysis study of six parasubstituted benzenediazonium salts, $X-C_6H_4N_2^+$ [X = $COOC_2H_5$, F, H, CH_3, OCH_3, and $N(CH_3)_2$], has been carried out in strongly acidic aqueous solution (1 M $HClO_4$), where the principal reductant is the hydrogen atom. Initially, H adducts of the diazonium salts are formed with rate constants of $(2.3-9.0) \times 10^8$ M^{-1} s^{-1}, followed by their decay to protonated aryl radicals without the intermediacy of the diazenyl radicals that are observed when the reductant is the solvated electron. After a deprotonation reaction, the thus formed aryl radicals attack the diazonium salt mainly at the terminal nitrogen atom to afford the radical cations of the corresponding azobenzenes, $(X-C_6H_4)_2N_2^{\bullet+}$, or eventually the corresponding OH adducts, $(X-C_6H_4)_2N_2OH^{\bullet}$, upon further reaction with water. For the dimethylamino substituent, the basicity is so high that the protonated radical cation of 4,4′-bis(dimethylamino)azobenzene is formed. Studies carried out at different pH values for this system lead to a determination of its pK_a = 2.0. For X = $COOC_2H_5$, F, H, and $N(CH_3)_2$, the rate-controlling step is the deprotonation reaction to afford the aryl radicals, whereas for X = CH_3 and OCH_3, it is the fragmentation of the H adduct to afford the protonated aryl radical. The characteristics of the corresponding OH adducts of the diazonium salts are also described briefly.

Introduction

Arenediazonium salts, ArN_2^+, are among the most useful reagents in organic chemistry,[1−4] because the versatile diazo group can be replaced by numerous other groups. This so-called dediazoniation reaction can take place both via a heterolytic pathway characterized by the intermediacy of aryl cations and a homolytic pathway involving aryl radicals. The homolytic pathway is depicted in Scheme 1, where the diazonium salt is reduced to the corresponding diazenyl radical, $ArN_2^{\bullet}$, by an appropriate electron-transfer agent, before the aryl radical, $Ar^{\bullet}$, is formed through the expulsion of dinitrogen.

In the most recent mechanistic studies, the focus has mainly been on the heterolytic processes,[5−11] whereas less attention has been paid to the homolytic counterparts[12−15] despite their great importance. One of the major difficulties associated with the investigation of homolytic processes is the extremely high reactivity of the diazenyl and aryl radicals produced as intermediates. For instance, in the classical Sandmeyer reaction, where the cuprous ion is used as electron-transfer agent, the aryl radicals produced are intercepted quite effectively in ligand-transfer reactions involving cupric salts, preventing further studies.

In our previous study on a series of parasubstituted benzenediazonium salts, $X-C_6H_4N_2^+$, we employed as electron-transfer agent the solvated electron, e_{aq}^-, generated in pulse radiolysis.[16] The solvated electron is the simplest, yet one of the most powerful reductants (oxidation potential = −2.86 V vs NHE).[17]

SCHEME 1

$$ArN_2^+ \xrightarrow{\text{electron transfer}} ArN_2^{\bullet} \longrightarrow Ar^{\bullet} + N_2$$

This allowed us to form the aryl radicals selectively and study the kinetic features of the reactions involving aryl radicals and diazonium salts. The kinetic analysis led to the proposal of the following mechanism, eqs 1−6:

$$e_{aq}^- + X-C_6H_4N_2^+ \xrightarrow{k_1} X-C_6H_4N_2^{\bullet} \quad (1)$$

$$X-C_6H_4N_2^{\bullet} + X-C_6H_4N_2^+ \underset{k_{-2}}{\overset{k_2}{\rightleftharpoons}} (X-C_6H_4)_2N_4^{\bullet+} \quad (2)$$

$$X-C_6H_4N_2^{\bullet} \xrightarrow{k_3} X-C_6H_4^{\bullet} + N_2 \quad (3)$$

$$X-C_6H_4^{\bullet} + X-C_6H_4N_2^+ \xrightarrow{k_4} (X-C_6H_4)_2N_2^{\bullet+} \quad (4)$$

$$(X-C_6H_4)_2N_2^{\bullet+} + H_2O \underset{k_{-5}}{\overset{k_5}{\rightleftharpoons}} (X-C_6H_4)_2N_2OH^{\bullet} + H^+ \quad (5)$$

$$\text{radicals} + \text{radical cations} \xrightarrow{k_6} \text{products} \quad (6)$$

In the first step, eq 1, e_{aq}^- reduces $X-C_6H_4N_2^+$ to the corresponding aryldiazenyl radical, $X-C_6H_4N_2^{\bullet}$. This radical is either involved in an equilibrium reaction with the diazonium salt, eq 2, in which a $(X-C_6H_4)_2N_4^{\bullet+}$ adduct is formed in a first substrate-dependent buildup, or it decays to the aryl radical, $X-C_6H_4^{\bullet}$, through the expulsion of dinitrogen, eq 3. Subsequently, $X-C_6H_4^{\bullet}$ is involved in a second substrate-dependent buildup, eq 4, where the radical cation of the corresponding azobenzene, $(X-C_6H_4)_2N_2^{\bullet+}$, is formed. Thus, it is suggested

* To whom correspondence should be addressed. E-mail: kdaa@chem.au.dk.
† University of Aarhus.
‡ Risø National Laboratory.
§ Present address: Strandhøjen 5, 4000 Roskilde.

10.1021/jp0273732 CCC: $25.00
Published on Web 05/13/2003

that the main attack occurs at the diazo group rather than at the aromatic ring in the diazonium salt. The radical cation, which is observable only for the strongest electron-donating substituents such as methoxy and dimethylamino, reacts with water to afford the corresponding OH adduct $(X-C_6H_4)_2N_2OH^{\bullet}$, eq 5. Other decay pathways are different second-order reactions pertaining to any of the radicals or radical cations present in the solution, eq 6.

In the present paper, our aim is to investigate in greater detail the reduction features of the very same parasubstituted benzenediazonium salts [$X-C_6H_4N_2^+BF_4^-$, X = $COOC_2H_5$, F, H, CH_3, OCH_3, and $N(CH_3)_2$] by employing the other strong and almost as simple reductant generated in pulse radiolysis, the hydrogen atom $H^{\bullet}$ (oxidation potential = −2.31 V vs NHE).[17] Still, the reaction pathway might be different in this case because of the profound ability of $H^{\bullet}$ of attacking aromatic rings. Most measurements were carried out in 1 M $HClO_4$, i.e., at pH 0, because this allowed the generation of $H^{\bullet}$ from the reaction between e_{aq}^- and H^+. Clearly, this change of medium might also influence the mechanistic pathway, although it should be underlined that the dimethylamino group of $(CH_3)_2N-C_6H_4N_2^+$ is not protonated to form a dication even at pH 0 as revealed by the recording of UV-vis spectra at different pH values. Another interesting point to investigate is the influence of the substituent in the para position on the reaction kinetics. In the previous study, we observed for most reactions except eq 4 essentially no substituent effect. Because $HO^{\bullet}$ is formed in pulse radiolysis along with e_{aq}^- and $H^{\bullet}$, the characteristics of the OH adducts of the diazonium salts are also described briefly herein. The focus in this paper thus clearly differs from that in previous pulse radiolysis studies of diazonium salts,[18,19] where the purpose either has been to investigate second-order radical−radical processes by employing high radiation doses[18] or to initiate chain processes involving alcohols and radicals derived thereof.[19]

The radiation of water using high-energy electrons leads to the formation of the species shown in eq 7, where the radiation chemical yields of the three principal radicals are $G(e_{aq}^-) \approx G(HO^{\bullet}) \approx 2.8 \times 10^{-7}$ mol J^{-1} and $G(H^{\bullet}) \approx 0.6 \times 10^{-7}$ mol J^{-1}:[17]

$$H_2O \xrightarrow{\text{ionizing radiation}} e_{aq}^-, HO^{\bullet}, H^{\bullet}, H^+, H_2O_2, H_2 \qquad (7)$$

The solvated electron can be converted to $H^{\bullet}$ in a deoxygenated solution at low pH (eq 8, $k_8 = 2.3 \times 10^{10}$ M^{-1} s^{-1}) or to $HO^{\bullet}$ in a N_2O saturated solution (eq 9, $k_9 = 9.1 \times 10^9$ M^{-1} s^{-1}):[20]

$$e_{aq}^- + H^+ \xrightarrow{k_8} H^{\bullet} \qquad (8)$$

$$e_{aq}^- + N_2O\ (+ H_2O) \xrightarrow{k_9} HO^{\bullet} + N_2 + HO^- \qquad (9)$$

Under such conditions, the radiation yields become $G(H^{\bullet}) \approx 3.4 \times 10^{-7}$ mol J^{-1} and $G(HO^{\bullet}) \approx 5.6 \times 10^{-7}$ mol J^{-1}, respectively, or even slightly larger because the above fast reactions may take place in the spurs before homogeneous conditions are attained. The procedure for scavenging $HO^{\bullet}$, $H^{\bullet}$, and $X-C_6H_4^{\bullet}$ usually involves *tert*-butanol as depicted in eqs 10−12 ($k_{10} = 6.0 \times 10^8$ M^{-1} s^{-1}, $k_{11} = 1.7 \times 10^5$ M^{-1} s^{-1}, and $k_{12} = 6.6 \times 10^5$ M^{-1} s^{-1} for X = H):[20,21]

$$HO^{\bullet} + (CH_3)_3COH \xrightarrow{k_{10}} {}^{\bullet}CH_2(CH_3)_2COH + H_2O \qquad (10)$$

$$H^{\bullet} + (CH_3)_3COH \xrightarrow{k_{11}} {}^{\bullet}CH_2(CH_3)_2COH + H_2 \qquad (11)$$

$$X-C_6H_4^{\bullet} + (CH_3)_3COH \xrightarrow{k_{12}} {}^{\bullet}CH_2(CH_3)_2COH + X-C_6H_5 \qquad (12)$$

In most experiments of the present study, we had to accept the presence of $HO^{\bullet}$ because its scavenging would be accompanied by the scavenging of $X-C_6H_4^{\bullet}$ produced along the reaction pathway.

Experimental Section

The diazonium salts were prepared according to the general procedure described in ref 22. They were recrystallized from acetonitrile and diethyl ether before use. The procedure for synthezising (*E*)-4,4′-dimethoxyazobenzene[23] and (*E*)-4,4′-bis-(dimethylamino)azobenzene[24] is described in the references listed. All other chemicals—perchloric acid, *tert*-butanol, Ar, O_2, and N_2O—were of the highest commercially available purity. The solutions were prepared in 100-mL syringes using triply distilled water. The diazonium salts were dissolved in the aqueous solution at the very last moment before the pulse radiolysis experiment in order not to form the corresponding substituted phenols in hydrolysis reactions involving the diazo group. This was also the reason that the maximum concentration of the salts never exceeded 0.2 M. Hydrolysis of the ester group in $C_2H_5OOC-C_6H_4N_2^+$ to a carboxylic acid did not take place. It was also found that the dimethylamino group of $(CH_3)_2N-C_6H_4N_2^+$ was not protonated to form a dication even at pH 0 as revealed by the recording of UV-vis spectra at different pH values. The syringes were covered with tinfoil to avoid photolysis of the labile diazonium salts. The pulse radiolysis experiments were performed on Risø's HRC linear accelerator which delivered 10-MeV electrons in a single pulse with a maximum intensity of 1 A. The dose, which was determined with the ferrocyanide dosimeter using $\epsilon_{420} = 1000$ M^{-1} cm^{-1} and $G = 6.0 \times 10^{-7}$ mol J^{-1}, was in most cases 0.8−40 Gy in 1-μs pulses. The cylindrical cell had a radius of 0.6 cm and a length of 2.55 cm. The light path length was 2 × 2.55 cm = 5.1 cm. The optical detection system consisted of a 150 W Varian high-pressure xenon lamp with increased intensity in short pulses, a Perkin-Elmer double quartz prism monochromator, and a Hamamatsu R955 photomultiplier. The data were recorded on a 125-MHz LeCroy 9400 digital oscilloscope and were transferred to a PC for further treatment.[25] The program Gepasi 3.21 was employed in the simulations of the kinetic traces.[26] In the steady-state radiolysis, a ^{60}Co radiation source was used with a dose rate of 260 krad/hour. After 1−3 h of radiation, the solutions were extracted three times with diethyl ether. The combined ether phases were washed with water, dried over molecular sieves, evaporated to a volume of 1 mL, and analyzed by GC-MS (HP 6890). The response factors were assumed to be one in the determination of the relative yields. All measurements were carried out at 20 °C.

Results and Discussions

Reactions Involving $H^{\bullet}$. Figure 1 shows characteristic kinetic traces in terms of plots of the optical density (OD) versus time (*t*) recorded for $C_6H_5N_2^+$ in strongly acidic medium at pH 0, where $H^{\bullet}$ is the only reductant present. For comparison, we have included as inset a trace recorded in neutral solution, where the solvated electron acts as the principal reductant.[16] One of the most distinct differences in the kinetic features for the two cases is the much larger spike observed at pH 0, which accordingly must be attributed to the formation and decay of the H adduct of the diazonium salt. Note that in neutral solution a minor

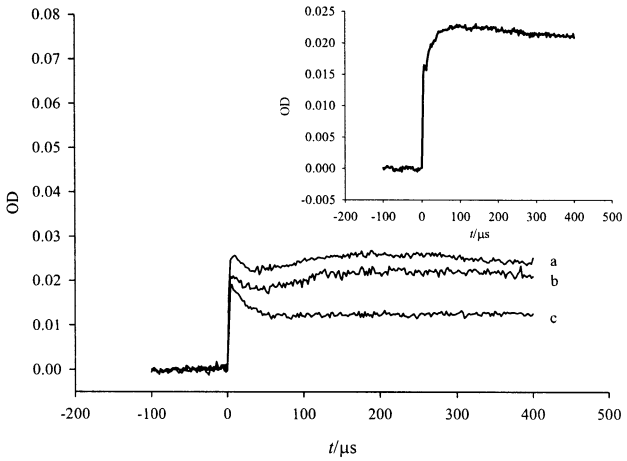

Figure 1. Traces of the transients recorded at 410 nm after a 2.5-Gy pulse on Ar-saturated pH 0 solutions of $C_6H_5N_2^+BF_4^-$: (a) 10^{-2}, (b) 5×10^{-3}, and (c) 10^{-3} M. Inset: Trace of the transients recorded at 410 nm after a 2.5-Gy pulse on an Ar-saturated neutral solution of 10^{-2} M $C_6H_5N_2^+BF_4^-$ (from ref 16).

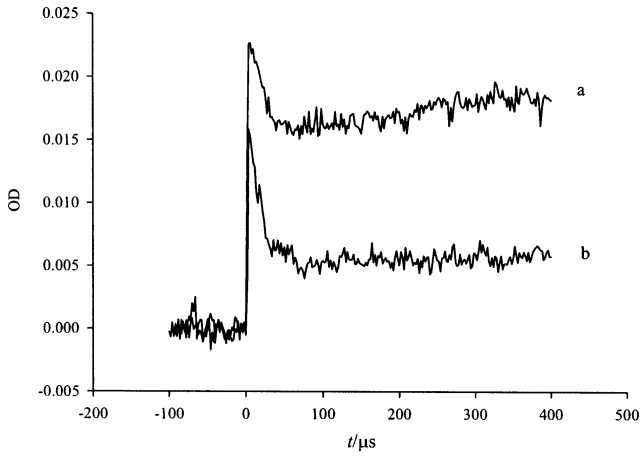

Figure 2. Traces of the transients recorded at 410 nm after a 2.5-Gy pulse on an Ar-saturated pH 0 solution of 2.5×10^{-3} M $C_6H_5N_2^+BF_4^-$: (a) without *tert*-butanol and (b) with 0.3 M *tert*-butanol.

amount of the H adduct is also formed ($\sim^1/_6$th of the amount formed at pH 0) along with the $(X-C_6H_4)_2N_4^{\bullet+}$ species, eq 2.[16]

In both neutral and acidic solutions, the hydroxyl radicals generated upon radiation will react fast with the diazonium salts to afford OH adducts, the spectra of which are located in the same wavelength region as those of the H adducts (see below). However, the exclusive formation of the H adducts can be achieved by taking advantage of the simple fact that $HO^\bullet$ is scavenged much more effectively than $H^\bullet$ by *tert*-butanol ($k_{10}/k_{11} = 3500$). This is illustrated in Figure 2, where the spike clearly becomes smaller but much more distinct upon adding 0.3 M *tert*-butanol to the acidic solution; additional *tert*-butanol has no further effect.

As to the second buildup occurring at larger time scales, it is slower in acidic than neutral solution. In neutral solution, this buildup for $X = OCH_3$ and $N(CH_3)_2$ was attributed to the formation of the radical cation of the corresponding azobenzenes, $(X-C_6H_4)_2N_2^{\bullet+}$, in the reaction between $X-C_6H_4^\bullet$ and $X-C_6H_4N_2^+$, eq 4.[16] For the other substituents, $(X-C_6H_4)_2N_2^{\bullet+}$ was not observable as it was transformed immediately to the corresponding OH adduct, $(X-C_6H_4)_2N_2OH^\bullet$, upon further reaction with water. That this is so also in acidic solution is substantiated by the fact that the same spectra are obtained

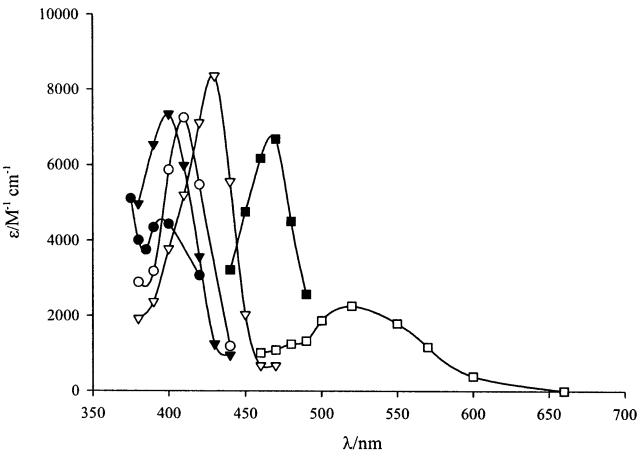

Figure 3. Absorption spectra of $X-C_6H_4N_2H^{\bullet+}$ for $X = COOC_2H_5$ (●), F (○), H (▼), CH_3 (▽), OCH_3 (■), and $N(CH_3)_2$ (□) recorded at pH 0 for diazonium salt concentrations larger than 10^{-2} M and in the presence of 0.3−1 M *tert*-butanol.

independent of pH although the substituent $X = N(CH_3)_2$ exhibits some distinctive features as described below. Note also that the second buildup is absent in the presence of *tert*-butanol (see Figure 2) because of the scavenging of $X-C_6H_4^\bullet$, eq 12. The relevant spectra of $(X-C_6H_4)_2N_2^{\bullet+}$ and $(X-C_6H_4)_2N_2OH^\bullet$ are collected in our previous paper.[16]

On the other hand, it is also clear that the mechanism for the generation of these species must be different at low pH because of the slower reaction kinetics observed, when the reductant is $H^\bullet$ rather than e_{aq}^-. Our working hypothesis is that the scheme outlined in eqs 13−15 followed by eqs 4−6 provides an adequate description of the reactions initiated by $H^\bullet$.

$$H^\bullet + X-C_6H_4N_2^+ \xrightarrow{k_{13}} X-C_6H_4N_2H^{\bullet+} \quad (13)$$

$$X-C_6H_4N_2H^{\bullet+} \xrightarrow{k_{14}} X-C_6H_4H^{\bullet+} + N_2 \quad (14)$$

$$X-C_6H_4H^{\bullet+} \xrightarrow{k_{15}} X-C_6H_4^\bullet + H^+ \quad (15)$$

The buildup of the H adduct $X-C_6H_4N_2H^{\bullet+}$, eq 13, is followed by its decay to afford the protonated aryl radical, $X-C_6H_4H^{\bullet+}$, through the expulsion of dinitrogen as depicted in eq 14. After the deprotonation reaction shown in eq 15, the thus formed $X-C_6H_4^\bullet$ is involved in the reactions of eqs 4−6 known from neutral solution.[16] Below, a detailed description of the proposed reaction scheme is provided.

Kinetics of eq 13. The H adducts are easily characterized through a study of the initial fast buildup. The spectra are shown in Figure 3. As expected, the absorption maximum is shifted toward longer wavelengths for the electron-donating groups. The spectral features alone do not allow us to decide if the attack takes place at the aromatic system or the diazo group. For $X = COOC_2H_5$, CH_3, OCH_3, and in particular $N(CH_3)_2$, there is even the possibility of abstracting a hydrogen atom from the ethyl or methyl groups as known from the reactions of methylated benzenes[25] and *N*,*N*-dimethylaniline with $HO^\bullet$.[27] It would be expected that $H^\bullet$ should be less reactive in this respect, but it is noteworthy that the determined extinction coefficients, ϵ, are particularly small for $X = N(CH_3)_2$ as seen in Figure 3. Accordingly, we emphasize that they should be considered as minimum values in this case.

The rate constants k_{13} determined from the pseudo-first-order buildups are collected in Table 1. The values vary from $2.3 \times$

TABLE 1: Rate Constants for the Reactions Involving H and OH Adducts of Parasubstituted Benzenediazonium Salts and (Protonated) Aryl Radicals[a]

X	k_{13} 10^8 M^{-1} s^{-1}	k_{14} 10^4 s^{-1}	k_{15}[b] 10^4 s^{-1}	k_4[c] 10^6 M^{-1} s^{-1}	k_{20} 10^8 M^{-1} s^{-1}
$COOC_2H_5$	3.3	40	0.7	1.5	15
F	5.0	7	0.6	1.3	2.0
H	5.8	7	1.3	6.3	4.1
CH_3	3.4	3	>3	9.0	6.2
OCH_3	2.3	5	>5	28[d]	35
$N(CH_3)_2$	9.0	2[e]	0.3[e]	59	47

[a] The uncertainty on the determination of the rate constants is 20%. [b] Determined from the kinetics of the buildup of $(X-C_6H_4)_2N_2^{\bullet+}$ or $(X-C_6H_4)_2N_2OH^{\bullet}$. [c] From ref 16 (denoted k_{11} therein), in neutral solution. [d] At pH 0, we find $k_4 = 1.9 \times 10^7$ M^{-1} s^{-1}. [e] See discussion in text concerning protonation of the dimethylamino group at pH 0.

10^8 M^{-1} s^{-1} for X = OCH_3 to 9.0×10^8 M^{-1} s^{-1} for X = $N(CH_3)_2$, which are comparable to those found for the reaction of $H^{\bullet}$ with other aromatic systems.[25,27,28] The reaction rates are relatively independent of the substituent, taking into account that the large k_{13} measured for X = $N(CH_3)_2$ possibly should find its origin in the competing hydrogen abstraction reaction.

Kinetics of eq 14. The fragmentation reaction of the H adducts $X-C_6H_4N_2H^{\bullet+}$ was studied as shown in Figure 2 in the presence of *tert*-butanol in order to scavenge the hydroxyl radicals generated initially and the aryl radicals generated in eq 15 (see eqs 10 and 12). The decay follows a simple first-order pathway attributed to the formation of the protonated aryl radical, $X-C_6H_4H^{\bullet+}$, through the expulsion of dinitrogen, eq 14. The reason that it is necessary to invoke the presence of this intermediate in strongly acidic solution prior to the formation of the corresponding aryl radical is that the kinetics of the formation of $(X-C_6H_4)_2N_2^{\bullet+}$ or $(X-C_6H_4)_2N_2OH^{\bullet}$ in the follow-up reactions of eqs 4 and 5 as mentioned is substantially slower at pH 0 than in neutral solution (see Figure 1). A decay of $X-C_6H_4N_2H^{\bullet+}$ to afford the corresponding aryldiazenyl radical, $X-C_6H_4N_2^{\bullet}$, can be excluded because of the lack of the characteristic buildup of $(X-C_6H_4)_2N_4^{\bullet+}$ known from neutral solution, eq 2.[16]

As to the structure of $X-C_6H_4H^{\bullet+}$, we find it unlikely that it should be a π complex. First of all, a ^{13}C NMR study of the benzenium ion generated in a $SbF_5-FSO_3H-SO_2ClF$ solution has revealed that this ion exists as a σ adduct,[29] although the π-complex structure presumably is the most stable one in the gas phase.[30] In addition, UV-vis spectra recorded herein for compounds such as benzene, toluene, and anisole in aqueous solution showed no changes upon lowering pH from seven to zero. Second, the relatively long lifetime observed experimentally for $X-C_6H_4H^{\bullet+}$ (see below) would not be in accordance with the expected fleeting existence of a π complex. On this basis, we conclude that the initial attack by $H^{\bullet}$ at the diazonium salt occurs at the aromatic ring rather than the diazo group as this will make the subsequent formation of a σ adduct of $X-C_6H_4H^{\bullet+}$ from $X-C_6H_4N_2H^{\bullet+}$ straightforward upon the expulsion of dinitrogen.

The fragmentation rate constants k_{14} determined for $X-C_6H_4N_2H^{\bullet+}$ are listed in Table 1. In general, the substituent dependency is relatively weak as it also was seen for the corresponding series of $X-C_6H_4N_2^{\bullet}$.[16] Still, X = $COOC_2H_5$ presents an exception with a k_{14} value being about an order of magnitude larger. Possibly, this behavior is related to the fact that the attack by $H^{\bullet}$ at the aromatic ring of the diazonium salt occurs at positions determined by the directing effects of both the N_2^+ and X groups. Because $COOC_2H_5$ is without comparison the strongest electron-withdrawing group among the substituents studied, other positions might become activated for the attack by $H^{\bullet}$ in this case, thereby leading to a different structure of $X-C_6H_4N_2H^{\bullet+}$.

Kinetics of eqs 15 and 4−6. Next, we focus on the kinetics of the second buildup occurring at 50−400 μs in the traces of Figures 1 and 2, attributed to the formation of $(X-C_6H_4)_2N_2^{\bullet+}$ in eq 4 for X = OCH_3 and $N(CH_3)_2$ and the corresponding OH adduct, $(X-C_6H_4)_2N_2OH^{\bullet}$, in eq 5 for the remaining substituents.[16]

(a) X = $COOC_2H_5$, F, and H. In these three cases, the buildup rates are independent of the concentration of the diazonium salt in the range $10^{-3}-10^{-2}$ M, even if the buildup becomes hardly detectable at the lowest concentrations employed as illustrated for X = H in Figure 1. This indicates that the kinetic control is by eq 15, i.e., the deprotonation of $X-C_6H_4H^{\bullet+}$ to form $X-C_6H_4^{\bullet}$, rather than the substrate-dependent reaction between $X-C_6H_4^{\bullet}$ and $X-C_6H_4N_2^+$ in eq 4. The kinetic control cannot be by the reaction of eq 14 because the rate constants k_{14} determined from the fragmentation kinetics of $X-C_6H_4N_2H^{\bullet+}$ are 5−60 times larger than the apparent buildup rate constants.

The rate constants k_{15} extracted from the buildups are included in Table 1 along with the rate constants k_4 determined previously in neutral solution (denoted k_{11} in ref 16). On the assumption that there would be no pH dependency on k_4, we can calculate the k_{15}/k_4 ratios to be in the range $(2-5) \times 10^{-3}$ M at pH 0, indicating that there should be a possibility of inducing a shift in the kinetic control from eq 15 to eq 4 at the lowest concentrations employed. Unfortunately, the measurements were made difficult by the smallness of the signals recorded under such conditions (see Figure 1), and no clear-cut evidence of a shift could be observed. At the same time, a systematic analysis of the effect of increasing pH on the kinetics was made impossible by the presence of the fast reaction occurring between e_{aq}^- and $X-C_6H_4N_2^+$ in eq 1 ($k_1 \sim (5-6) \times 10^{10}$ M^{-1} s^{-1}) at large pH. However, until pH 2, no changes were detected in the reaction kinetics.

(b) X = CH_3. For the methyl substituent, the buildup was composed of two components with the first one being independent of diazonium salt concentration and equal to 3×10^4 s^{-1}. On top of the first part, a slower and not easily detectable concentration-dependent part pertaining to eq 4 appeared when concentrations below 10^{-3} were employed; at larger concentrations, the two components merged to one with the buildup rate constant still being equal to 3×10^4 s^{-1}. Because this value corresponds exactly to the value of k_{14} measured for the fragmentation reaction of $X-C_6H_4N_2H^{\bullet+}$, we suggest that the first component simply is the buildup of $X-C_6H_4H^{\bullet+}$, thus providing a more direct proof for its existence. The above observations also imply that the rate constant k_{15} in this case must be larger than 3×10^4 s^{-1}.

(c) X = OCH_3. When the substituent is a methoxy group, the apparent buildup rate constant k_{app} is dependent on the diazonium salt concentration as shown by the plot in the inset of Figure 4. Actually, this plot with the appearance of an asymptote at the highest concentrations employed is quite similar to the one obtained in neutral solution (see Figure 4 in ref 16). However, the origin of the asymptotes is different; while it in the case of e_{aq}^- as reductant is set by the lifetime of the diazenyl radical ($k_3 = 1 \times 10^5$ s^{-1}),[16] it is in the case of $H^{\bullet}$ as reductant set by the lifetime of either $X-C_6H_4N_2H^{\bullet+}$ or $X-C_6H_4H^{\bullet+}$. Because the decay measurements of $X-C_6H_4N_2H^{\bullet+}$ provided a value of $k_{14} = 5 \times 10^4$ s^{-1} which is equal to the present asymptotic value, we conclude that the rate-controlling step pertains to eq 14 and accordingly $k_{15} > 5 \times 10^4$ s^{-1}. It is

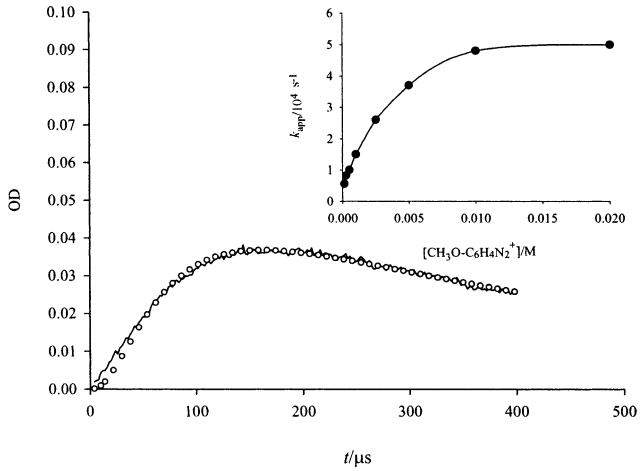

Figure 4. Trace of the transient $(CH_3O-C_6H_4)_2N_2^{\bullet+}$, recorded at 620 nm after a 1-Gy pulse on an Ar-saturated pH 0 solution of 10^{-3} M $CH_3O-C_6H_4N_2^+BF_4^-$. The curve (○) shows the fit to the reaction scheme, eqs 13−15 and 4−6, with the following rate constants ensuing: $k_4 = 1.9 \times 10^7$ M^{-1} s^{-1}, $k_{5/6} = 2000$ s^{-1}, $k_{13} = 2.3 \times 10^8$ M^{-1} s^{-1}, and $k_{14} = 5 \times 10^4$ s^{-1}. Equation 15 is assumed to be fast and without influence on the kinetics. Inset: Apparent rate constant k_{app} of buildup of $(CH_3O-C_6H_4)_2N_2^{\bullet+}$ as a function of the diazonium salt concentration.

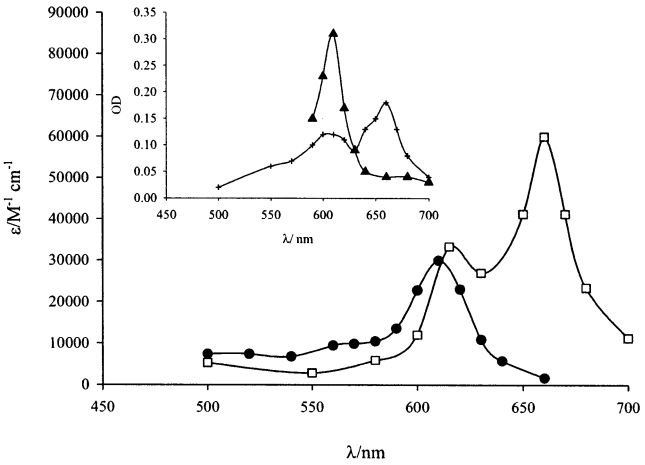

Figure 5. Absorption spectra of the species obtained as the result of the slow buildup for $X = N(CH_3)_2$ in a pH 0 (●) and a neutral solution (□). The latter spectrum is taken from ref 16. Inset: Absorption spectra of the radical cation of (*E*)-4,4′-bis(dimethylamino)azobenzene (+) taken from ref 16 and the protonated radical cation generated after a 10-Gy pulse on an Ar-saturated pH 0 solution containing 5×10^{-4} M of the parent azo compound (▲). In the latter case, the spectrum has been corrected for the contribution from the pertinent H adduct recorded in the presence of *tert*-butanol.

surprising that the k_{15} values obtained for $X = OCH_3$ and CH_3 should be so much larger than the corresponding values of (0.6−1.3) $\times 10^4$ s^{-1} obtained for $X = COOC_2H_5$, F, and H; that is, the deprotonation reaction should become faster as the electron-donating power of the substituent increases. One simple explanation for this behavior is that the structure of the protonated aryl radical is not the same for the different substituents as it depends on the exact site at which the initial attack by H$^\bullet$ at the diazonium salt occurred. Indeed, the fragmentation kinetics of $X-C_6H_4N_2H^{\bullet+}$ also provided indications of such structural differences as discussed above.

It should be underlined that the values of the apparent pseudo-first-order rate constants given in the inset of Figure 4 are only rough estimations. To extract all relevant kinetic parameters with less uncertainty simulations of the complete reaction scheme using the program Gepasi 3.21 were required.[26] The slope of the above plot determined at low concentrations was used as input value for k_4, whereas k_{14} was put equal to the asymptotic value of 5×10^4 s^{-1}. The previously determined value of $k_{13} = 2.3 \times 10^8$ M^{-1} s^{-1} was kept fixed. An example of a fit is illustrated in Figure 4 providing the rate constant k_4 as well as the overall rate constant for the decay pertaining to eqs 5 and 6, denoted $k_{5/6}$. Note that the value of $k_4 = 1.9 \times 10^7$ M^{-1} s^{-1} is in reasonable agreement with the corresponding rate constant of 2.8×10^7 M^{-1} s^{-1} obtained in neutral solution, showing that the pH effect on eq 4 is small.

According to the reaction scheme, $k_{5/6}$ should be a composite of mixed-order rate constants, and indeed, dose variation experiments revealed that the first-order decay was partly mixed with second-order processes at high doses. However, for the sake of computational simplicity, the values of $k_{5/6}$ were assumed to be first-order in all calculations (and thus given in units of s^{-1}). In general, $k_{5/6}$ was confined to the range 500−2000 s^{-1}, showing some variations from one experiment to another. The values of the corresponding decay rate constant of 1000−3000 s^{-1} obtained in neutral solution (denoted $k_{12/13}$ in ref 16) were slightly larger,[16] presumably because of less influence from the reverse reaction of eq 5.[25,27]

From a kinetic point of view, the results might also be interpreted in terms of an alternative mechanism, in which the reactions depicted in eqs 4 and 15 are replaced by the reactions given in eqs 16 and 17.

$$X-C_6H_4H^{\bullet+} + X-C_6H_4N_2^+ \xrightarrow{k_{16}} X-C_6H_4H^+N_2C_6H_4-X^{\bullet+} \quad (16)$$

$$X-C_6H_4H^+N_2C_6H_4-X^{\bullet+} \xrightarrow{k_{17}} (X-C_6H_4)_2N_2^{\bullet+} + H^+ \quad (17)$$

In this mechanism, the protonated aryl radical attacks the diazonium salt in eq 16, followed by a deprotonation reaction of the generated intermediate to afford the radical cation of the pertinent azobenzene in eq 17. For $X = OCH_3$, the rate-controlling step would be eq 16, and for $X = COOC_2H_5$, F, and H, it would be eq 17, whereas the kinetic control would be mixed for $X = CH_3$. The weakness of such an interpretation, however, is its implication at least in the case of $X = OCH_3$ that the reactivity of the protonated aryl radical toward the diazonium salt should be essentially the same as that of the aryl radical itself. Clearly, this seems unlikely, and we therefore consider the alternative mechanism as implausible.

(d) X = N(CH$_3$)$_2$. The dimethylaminobenzenediazonium salt turned out to be a particular case due to the basicity of the $N(CH_3)_2$ substituent. Although the salt itself is not protonated at pH 0 because of the presence of the strongly electron-withdrawing N_2^+ group, this may happen for some of the intermediates of higher base strength produced along the reduction pathway. For instance, the pK_a of the protonated dimethylaminophenyl radical should be comparable with that of *N*,*N*-dimethylanilinium (pK_a = 5.15),[31] so at low pH, an immediate protonation of the dimethylamino group would be predicted to take place.

A clear indication of that indeed being the case came as the spectrum recorded for the radical cation formation with maxima at ca. 610 and 660 nm in neutral solution was replaced by a spectrum having its maximum at 610 nm at pH 0 as shown in Figure 5. Moreover, the buildup of this new species occurred slowly with an apparent rate constant of 3×10^3 s^{-1}, independent of diazonium salt concentration and pH in the interval 0−4. In neutral solution, the buildup was found to be

dependent on the concentration with $k_4 = 5.9 \times 10^7\ M^{-1}\ s^{-1}$.[16] The overall kinetic behavior is thus similar to that observed for the electron-withdrawing substituents, substantiating the view that the dimethylamino group at this point has been protonated to form the dimethylammonium group.

In our previous study, the intermediate detected in neutral solution was attributed to the radical cation of (*E*)-4,4′-bis(dimethylamino)azobenzene,[16] and accordingly, we assign the new spectrum obtained at pH 0 to the protonated radical cation of (*E*)-4,4′-bis(dimethylamino)azobenzene. This assignment was validated by generating the very same radical cations in alternative pathways involving oxidation of the parent azo compound. In neutral solution, this oxidation process could be carried out quite easily using an oxidant such as Tl^{2+} (generated from $Tl^+ + HO^\bullet$) and in strongly acidic solution through the formation of the OH adducts of the azo compound followed by elimination of water as illustrated in eq 18.[16,25,27,28,32−35]

$$X{-}C_6H_4N{=}NC_6H_4\text{-}XOH^\bullet + H^+ \rightleftharpoons X{-}C_6H_4N{=}NC_6H_4\text{-}X^{\bullet+} + H_2O \quad (18)$$

Note that the above reaction is the same as that given in eq 5. In neutral solution, the extremely low solubility of (*E*)-4,4′-bis(dimethylamino)azobenzene (presumably in the μM range) made the calculation of the extinction coefficient of the generated radical cation impossible because of incomplete scavenging as described elsewhere.[16] No such solubility problems were encountered at pH 0 with one of the dimethylamino groups of (*E*)-4,4′-bis(dimethylamino)azobenzene being protonated.[36]

The inset of Figure 5 shows the spectra of the radical cations of the azo compound in both neutral and pH 0 solutions. In neutral solution, an absorption spectrum with the characteristic peaks at ca. 610 and 660 nm is obtained in agreement with the corresponding spectrum recorded upon the pulse radiolytic reduction of the diazonium salt (see Figure 5).[16] The minor peak is shifted slightly and the peak ratio is different, but this we attribute to the uncertainties associated with carrying out experiments on extremely low concentrations of the azo compound. In addition, there may be a small contribution from the pertinent H adduct. At pH 0, exactly the same feature is observable as in the case of the diazonium salt; that is, the peak at 610 nm is the only one present. On this basis, we conclude that the identity of the intermediate indeed is the protonated radical cation of 4,4′-bis(dimethylamino)azobenzene. It should be noted that a calculation of its extinction coefficient at 610 nm apparently would lead to a smaller value of 21 000 M^{-1} cm^{-1} than the 30 000 M^{-1} cm^{-1} determined when it has been generated through the diazonium salt pathway (see Figure 5). However, this is probably due to a lower than expected yield of the OH adduct depicted in eq 18 because of the presence of a competing hydrogen abstraction reaction between $HO^\bullet$ and the dimethylamino group. For instance, in the reaction between $HO^\bullet$ and *N*,*N*-dimethylaniline, such a pathway has been shown to constitute as much as 30%.[27,36]

With this protonation reaction in mind, it now becomes possible to encompass the $X = N(CH_3)_2$ case in the general reaction scheme outlined for the other compounds. Following either the formation of the H adduct in eq 13 or the protonated aryl radical in the subsequent step, a fast protonation of the dimethylamino group will take place. From this moment on, the substituent becomes the electron-withdrawing dimethylammonium group rather than the electron-donating dimethylamino group. Thus, the rate-controlling step occurring with a rate

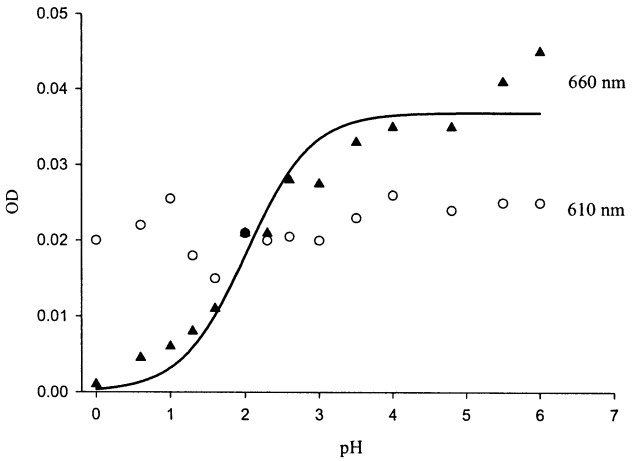

Figure 6. Optical density of the radical cation and the protonated radical cation of (*E*)-4,4′-bis(dimethylamino)azobenzene measured at 660 (▲) and 610 nm (○) after a 20-Gy pulse on an Ar-saturated solution of 10^{-4} M $(CH_3)_2N{-}C_6H_4N_2^+BF_4^-$ as a function of pH.

constant of $3 \times 10^3\ s^{-1}$ is the deprotonation of $(CH_3)_2N^+H{-}C_6H_4H^{\bullet+}$ to $(CH_3)_2N^+H{-}C_6H_4^\bullet$ in eq 15. In comparison, $k_{15} = (6{-}7) \times 10^3\ s^{-1}$ for X = F and $COOC_2H_5$. This also implies that the follow-up reaction in terms of the attack by $(CH_3)_2N^+H{-}C_6H_4^\bullet$ on $(CH_3)_2N{-}C_6H_4N_2^+$ to form the corresponding protonated azobenzene radical cation in eq 4 has to be fast with a rate constant larger than $10^7\ M^{-1}\ s^{-1}$. The latter does not seem implausible as the corresponding reaction between $(CH_3)_2N{-}C_6H_4^\bullet$ and $(CH_3)_2N{-}C_6H_4N_2^+$ in neutral solution proceeds with a rate constant of $5.9 \times 10^7\ M^{-1}\ s^{-1}$.[16]

An interesting aspect of the above interpretation is the transformation of the protonated radical cation of (*E*)-4,4′-bis(dimethylamino)azobenzene with the characteristic absorption band at 610 nm into the deprotonated radical cation at higher pH with its strong band at 660 nm (eq 19).

$$(CH_3)_2N^+H{-}C_6H_4N{=}NC_6H_4{-}N(CH_3)_2^{\bullet+} + H_2O \rightleftarrows (CH_3)_2N{-}C_6H_4N{=}NC_6H_4\text{-}N(CH_3)_2^{\bullet+} + H_3O^+ \quad (19)$$

In Figure 6, the measured OD(660 nm) and OD(610 nm) values are plotted against $pH^\bullet$. As seen, there is a pronounced increase in OD(660 nm) as a function of pH due to the increasingly larger amount of deprotonated radical cation formed. The lack of variation in OD(610 nm) is due to the simple fact that the extinction coefficients of the radical cation and its protonated form are essentially the same at $\lambda = 610$ nm. From this plot, the pK_a of the protonated radical cation of (*E*)-4,4′-bis(dimethylamino)azobenzene is easily extracted at the midpoint to be 2.0 ± 0.2. In comparison, the pK_a's of double protonated (*E*)-4,4′-bis(dimethylamino)azobenzene have been found to be equal to 1.5 and 3.2, respectively.[37]

Reactions Involving $HO^\bullet$. Even if the focus of the present and the previous work[16] has been on the reduction of diazonium salts using the hydrogen atom and the solvated electron, it is still important to pay attention to the reactions of the hydroxyl radicals and their possible influence on the reaction kinetics for the other species. The hydroxyl radicals are formed initially along with the other two species and because they could not be scavenged easily by adding *tert*-butanol without also scavenging the aryl radicals generated along the pathway we had to accept their presence.

The reaction chemistry of hydroxyl radicals can be studied selectively in pulse radiolysis by employing N_2O-saturated solutions, where e_{aq}^- is converted to $HO^\bullet$ through eq 9. The

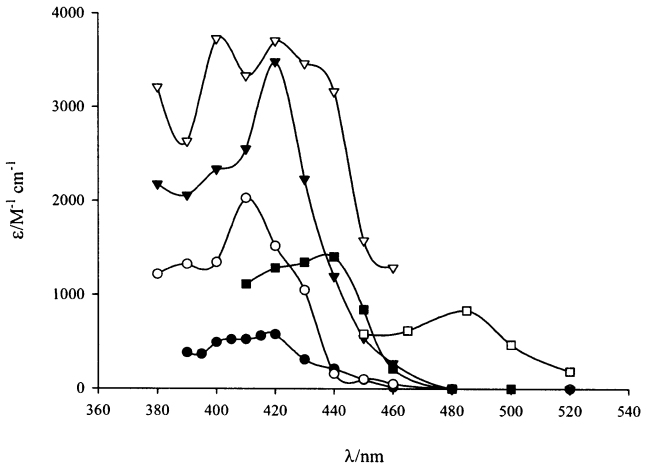

Figure 7. Absorption spectra of $X-C_6H_4N_2OH^{\bullet+}$ for X = $COOC_2H_5$ (●), F (○), H (▼), CH_3 (▽), OCH_3 (■), and $N(CH_3)_2$ (□) recorded in N_2O-saturated neutral solutions. The spectra have been corrected for the contribution from the H adducts.

initial reaction occurring between $HO^{\bullet}$ and the diazonium salts to afford the OH adduct, $X-C_6H_4N_2OH^{\bullet+}$, is depicted in eq 20.

$$HO^{\bullet} + X-C_6H_4N_2^{+} \xrightarrow{k_{20}} X-C_6H_4N_2OH^{\bullet+} \qquad (20)$$

In Figure 7, the spectra of $X-C_6H_4N_2OH^{\bullet+}$ are shown. As it was the case for the H adducts, we do not know at which position(s) the addition of $HO^{\bullet}$ occurs. For the substituents X = $COOC_2H_5$, CH_3, OCH_3 and in particular $N(CH_3)_2$, there is even the possibility of having a hydrogen abstraction reaction, well-known from the radiation chemistry of methylated benzenes[25] and *N*,*N*-dimethylaniline.[27] It was not possible to detect any such radicals as their spectra presumably are located in the absorption range of the diazonium salts themselves. Obviously, the generation of radicals would lead to an underestimation of the extinction coefficients of $X-C_6H_4N_2OH^{\bullet+}$ and provide an explanation why some of the spectra look relatively small and broad with shoulders. The values of k_{20} are all in the range $(0.2-4.7) \times 10^9$ M^{-1} s^{-1} with the fastest reactions occurring for X = $COOC_2H_5$, CH_3, OCH_3, and $N(CH_3)_2$. In fact, the number of 4.7×10^9 M^{-1} s^{-1} determined for X = $N(CH_3)_2$ is almost the same as that estimated for the hydrogen abstraction reaction between $HO^{\bullet}$ and *N*,*N*-dimethylaniline.[27]

We did not investigate in detail the decays of the OH adducts because our purpose in the present project was mainly to estimate their influence on the traces recorded for the reactions involving e_{aq}^- and $H^{\bullet}$ on the longer time scale, where the intermediates $(X-C_6H_4)_2N_2^{\bullet+}$ and $(X-C_6H_4)_2N_2OH^{\bullet}$ were formed. For the substituents OCH_3 and $N(CH_3)_2$ with λ_{max} of $(X-C_6H_4)_2N_2^{\bullet+}$ appearing above 600 nm, the effect of the OH adducts and radicals derived thereof could be neglected as there was no overlay of the spectra at all. The presence of the OH adducts will only manifest itself through a slightly enhanced rate of eq 6. For the remaining substituents, on the other hand, the situation was more complex, because the contribution from the OH adducts constituted as much as 10−50% of the total OD in the relevant wavelength range of 380−410 nm pertaining to the intermediate $(X-C_6H_4)_2N_2OH^{\bullet}$. Because the exact contribution was dependent on the diazonium salt concentration, we found it difficult to carry out a precise correction procedure, and accordingly, we had to accept the additional uncertainties introduced thereby in the measurements.[16]

Steady-State Radiolysis. A few steady-state radiolysis experiments using a ^{60}Co radiation have been carried out on the two diazonium salts with X = H and OCH_3. These included solutions with e_{aq}^- (10^{-2} M diazonium salt, Ar-saturated neutral solution) and $H^{\bullet}$ (10^{-2} M diazonium salt, Ar-saturated pH 0 solution) being the principal reductants, respectively. Note that $HO^{\bullet}$ will be present in both cases as well. Upon radiolysis, the aqueous solutions were extracted with diethyl ether and the products in the organic phase were analyzed qualitatively by means of GC-MS. For X = OCH_3, the main product (relative yield > 80%) detected was the corresponding (*E*)-4,4′-dimethoxyazobenzene ($m/z = 242$) as confirmed by comparison with an authentic sample of the compound. Minor amounts of arylated (*E*)-4,4′-dimethoxyazobenzene ($m/z = 348$) were also found. For X = H, the relative yield of (*E*)-azobenzene ($m/z = 182$) was lower (∼30%), and it was accompanied by quite substantial amounts of both mono- ($m/z = 258$) and diarylated azobenzene ($m/z = 334$). For both diazonium salts, there were traces of the dimer $(X-C_6H_4)_2$.

The arylated azo compounds may have their origin in several processes. One possibility is that the azobenzenes formed during radiolysis are attacked further by the aryl radicals. This pathway, however, is somewhat disfavored by the fact that the solubility of the azobenzenes is low. For a similar reason, it seems unlikely that the compounds should be formed in the second-order processes depicted in eq 6 involving radical and radical cations because the concentration of these reactive species would be low under steady-state conditions. A possible reaction pathway is that the OH adduct of the azobenzene, $(X-C_6H_4)_2N_2OH^{\bullet}$, formed in eq 5 reacts further with the diazonium salt to afford the arylated azo compounds upon elimination of water (and expulsion of dinitrogen). Alternatively, the arylation may take place at an earlier stage, if the initial attack by the aryl radical on the diazonium salt in eq 4 occurs at the aromatic ring rather than the diazo group. On the other hand, it should be noted that the spectral features of the intermediates generated in the pulse radiolysis experiments seem to be consistent with those of an OH adduct of azobenzene.[16]

Acknowledgment. We thank Hanne Corfitzen and Torben Johansen for skilful technical assistance. We are indebted to Dr. Mats Jonsson for carrying out some experiments for us on the pulse radiolysis equipment at the Royal Institute of Technology in Stockholm at the time when the pulse radiolysis facilities at Risø were shut down. The referees are thanked for valuable comments and *Statens Naturvidenskabelige Forskningsråd* for financial support.

References and Notes

(1) Wulfman, D. S. In *The Chemistry of Diazonium and Diazo Compounds*; Patai, S., Ed.; Wiley: Chichester, U.K., 1978.

(2) Zollinger, H. *Diazo Chemistry I, Aromatic and Heteroaromatic Compounds;* VCH: Weinheim, Germany, 1994.

(3) Zollinger, H. In *The Chemistry of Triple Bonded Functional Groups*; Patai, S., Rappoport, Z., Eds.; Wiley: Chichester, U.K., 1983.

(4) Galli, C. *Chem. Rev.* **1988**, *88*, 765.

(5) Barbero, M.; Degani, I.; Dughera, S.; Fochi, R. *J. Org. Chem.* **1999**, *64*, 3448.

(6) Bravo-Díaz, C.; Romsted, L. S.; Harbowy, M.; Romero-Nieto, M. E.; Gonzalez-Romero, E. *J. Phys. Org. Chem.* **1999**, *12*, 130.

(7) Steenken, S.; Ashokkumar, M.; Maruthamuthu, P.; McClelland, R. A. *J. Am. Chem. Soc.* **1998**, *120*, 11925.

(8) Cuccovia, I. M.; da Silva, M. A.; Ferraz, H. M. C.; Pliego, J. R., Jr.; Riveros, J. M.; Chaimovich, H. *J. Chem. Soc., Perkin Trans. 2* **2000**, 1896.

(9) Canning, P. S. J.; McCrudden, K.; Maskill, H.; Sexton, B. *J. Chem. Soc., Perkin Trans. 2* **1999**, 2735.

(10) Romero-Nieto, M. E.; Malvido-Hermelo, B.; Bravo-Díaz, C.; González-Romero, E. *Int. J. Chem. Kinet.* **2000**, *32*, 419.

(11) Costas-Costas, U.; Gonzalez-Romero, E.; Bravo-Díaz, C. *Helv. Chim. Acta* **2001**, *84*, 632.
(12) Kosynkin, D.; Bockman, T. M.; Kochi, J. K. *J. Am. Chem. Soc.* **1997**, *119*, 4846.
(13) Quintero, B.; Morales, J. J.; Quiros, M.; Martinéz-Puentedura, M. I.; del Carmen Cabeza, M. *Free Radical Biol. Med.* **2000**, *29*, 464.
(14) Geahigan, K. B.; Taintor, R. J.; George, B. M.; Meagher, D. A.; Nalli, T. W. *J. Org. Chem.* **1998**, *63*, 6141.
(15) Hanson, P.; Rowell, S. C.; Taylor, A. B.; Walton, P. H.; Timms, A. W. *J. Chem. Soc., Perkin Trans. 2* **2002**, 1126.
(16) Daasbjerg, K.; Sehested, K. *J. Phys. Chem A* **2002**, *106*, 11098.
(17) Spinks, J. W. T.; Woods, R. J. *Introduction to Radiation Chemistry*, 3rd ed.; Wiley: New York, 1990.
(18) Brede, O.; Mehnert, R.; Naumann, W.; Becker, H. G. O. *Ber. Bunsen-Ges. Phys. Chem.* **1980**, *84*, 666.
(19) Packer, J. E.; Mönig, J.; Dobson, B. C. *Aust. J. Chem.* **1981**, *34*, 1433.
(20) Buxton, G. V.; Greenstock, C. L.; Helman, W. P.; Ross, A. B. *J. Phys. Chem. Ref. Data* **1988**, *17*, 513.
(21) Fang, X.; Mertens, R.; von Sonntag, C. *J. Chem. Soc., Perkin Trans. 2* **1995**, 1033.
(22) Starkey, E. B. In *Organic Syntheses*; Wiley & Sons: New York, 1943; Collect. Vol II, p 225.
(23) Yamamoto, S.; Nishimura, N.; Hasegawa, S. *Bull. Chem. Soc. Jpn.* **1971**, *44*, 2018.
(24) Vorländer, D.; Wolferts, E. *Chem. Ber.* **1923**, *56*, 1229.
(25) Sehested, K.; Corfitzen, H.; Christensen, H. C.; Hart, E. J. *J. Phys. Chem.* **1975**, *79*, 310.
(26) *Gepasi*, version 3.21; Pedro Mendes, 1996−1999. The program may be downloaded from the Internet.
(27) Holcman, J.; Sehested, K. *J. Phys. Chem.* **1977**, *81*, 1963.
(28) O'Neill, P.; Steenken, S.; Schulte-Frohlinde, D. *J. Phys. Chem.* **1975**, *79*, 2773.
(29) Olah, G. A.; Staral, J. S.; Asencio, G.; Liang, G.; Forsyth, D. A.; Mateescu, G. D. *J. Am. Chem. Soc.* **1978**, *100*, 6299.
(30) Mason, R. S.; Williams, C. M.; Anderson, P. D. J. *J. Chem. Soc., Chem. Commun.* **1995**, 1027.
(31) *Handbook of Chemistry and Physics*; Lide, D. R., Ed.; CRC Press: Boca Raton, FL, 1991.
(32) Sehested, K.; Holcman, J.; Hart, E. J. *J. Phys. Chem.* **1977**, *81*, 1363.
(33) Sehested, K.; Hart, E. J. *J. Phys. Chem.* **1975**, *79*, 1639.
(34) Zevos, N.; Sehested, K. *J. Phys. Chem.* **1978**, *82*, 138.
(35) Holcman, J.; Sehested, K. *J. Phys. Chem.* **1976**, *80*, 1642.
(36) Note that it is unknown to which extent the determination of the value of $\epsilon = 30\,000\ M^{-1}\ cm^{-1}$ at 610 nm for the protonated radical cation in the diazonium salt pathway is influenced by a hydrogen abstraction reaction occurring between the dimethylamino group of the diazonium salt and $H^{\bullet}$ (see also Figure 3).
(37) Cilento, G. *J. Org. Chem.* **1959**, *24*, 2015.